Supporting Information

High-performance broadband polarization-sensitive photodetector based on BiSeS nanowires

Junda Yang [1], Fen Zhang [1], Shuo Liu [1], Xinyun Zhou [1], Jiacheng Yang[1], Qinglin Xia[1], Mianzeng Zhong[1](✉)
[1]Hunan Key Laboratory of Nanophotonics and Devices, School of Physics, Central South University, Changsha 410083, China.

*Corresponding Author E-mail: zmzhong@csu.edu.cn

Synthesis of $Bi_2Se_{2.33}S_{0.67}$ crystals

The used $Bi_2Se_{2.33}S_{0.67}$ crystals were prepared via chemical vapor transport (CVT) method, a classic technique which utilizes volatile transport reagents to facilitate the growth of bulk single crystals in a sealed container.[1] The raw materials contained high-purity Bi, Se and S powders (99.999%) at an atomic ratio of Bi/Se/S = 4:5:2 along with iodine power (5 mg/cm^3), and all of these were encapsulated in a sealed quartz tube with a vacuum condition of about 10^{-3} Pa. The tube was placed in a horizontal two-zone tube furnace, which has hot and cold zone used for the reaction and growth respectively. The hot and cold zone need be slowly heated to 700 °C and 640 °C respectively, which is required to maintain these temperatures for 4320min. Subsequently, the furnace was allowed to cool to 240 °C at a rate of 0.8 °C/h followed by cooling naturally to room temperature. Finally, shiny monocrystalline $Bi_2Se_{2.33}S_{0.67}$ nanowires with micron-scale length were obtained at the sink zone of the tube.

Fabrication of the device and preparation of the TEM sample

At first, $Bi_2Se_{2.33}S_{0.67}$ nanowires clusters were transferred onto the Si/SiO_2 substrates (the Si substrate covered with 285 nm SiO_2 insulating top layer) by tweezers, and pressed gently. A large number of dispersed nanowires were left on the surface of the substrates after removing the nanowire clusters. Then the Au film was tightly deposited on the surface of the whole nanowire by thermal evaporation to form

a pair of gold electrodes of the device. After that, the Au film serving as mask was gently removed, constructing the channel of the device. For TEM, HRTEM and SAED measurements, the sample was required to a pretreatment. Specifically, as-sythesized $Bi_2Se_{2.33}S_{0.67}$ nanowires were spin-coated with polymethyl methacrylate (PMMA) liquid with a rotating speed of 3000 r/s. After the PMMA film had been dried under vacuum conditions for 24 hours, it was immersed in the 1 M KOH solution to erode SiO_2 layer. As soon as the PMMA film containing $Bi_2Se_{2.33}S_{0.67}$ crystals was floated, it would be transferred onto the copper grid. In the end, the PMMA was dissolved in acetone, leaving the $Bi_2Se_{2.33}S_{0.67}$ on the copper grid.

Characterization methods

The crystallographic structure and chemical composition of the nanowires were examined via a transmission electron microscope (TEM, Spectra 300S, Thermo Fisher Scientific) and an Energy Disperse Spectroscopy detector. The morphology and thickness of the sample were observed using optical microscopy and Raman spectroscopy (InVia Qontor, Ranishaw). Raman spectra were collected from 50 to 300 cm^{-1} using 532 nm laser. The angle-resolved polarized Raman spectra were obtained by rotating a specially designed platform (loaded with our sample) clockwise at intervals of 10°. Meanwhile, a linear polarizer was inserted into the path of scattered light to realize parallel-configuration. The electrical experiments were carried out on a probe station, and data were collected with a semiconductor device analyzer (B2912A, Keysight Technologies). For polarization sensitive measurement, we built a home-made system, including Glan prism and Half-wave plate. The partially polarized laser was set to pass through a Glan-Thomson prism, which changed partially polarized light to linearly polarized light; and through half-wave plate, which changed the direction of linearly polarized light and then illuminated the device. The response speed of the photodetector was measured by a home-build system, which

consists of Laser, Galvo scanning system, Optical microscope, Device test socket, Current amplifier, Lock-in amplifier, and Oscilloscope.

Density Functional Theory Calculations.

The calculations are performed by using the projector augmented plane-wave (PAW) method[2, 3] within the framework of DFT in the Vienna ab initio Simulation Package (VASP).[4] The generalized gradient approximation (GGA) of Perdew, Burke, and Ernzerhof (PBE) functional[5] is adopted for electron exchange and correlation. The spin–orbit coupling effect is also considered in the calculation. A vacuum larger than 15 Å is used to eliminate the interaction between adjacent images. The cut off energy for the plane-wave basis set is set to 500 eV.[6] In the total energy calculations, a set of (12 × 12 × 1) k-point samplings was used for Brillouin zone integration.[7] All of the structures are fully relaxed with a force tolerance of 0.01 eV/Å.

Figures and tables

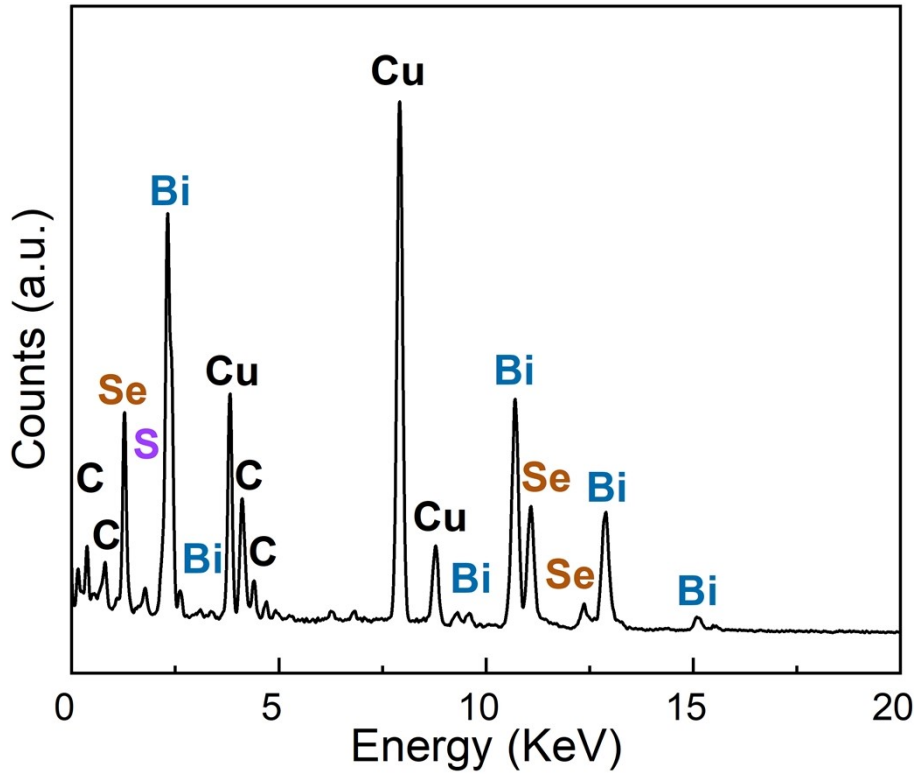

Figure S1 EDS analysis of the $Bi_2Se_{2.33}S_{0.67}$ nanowire.

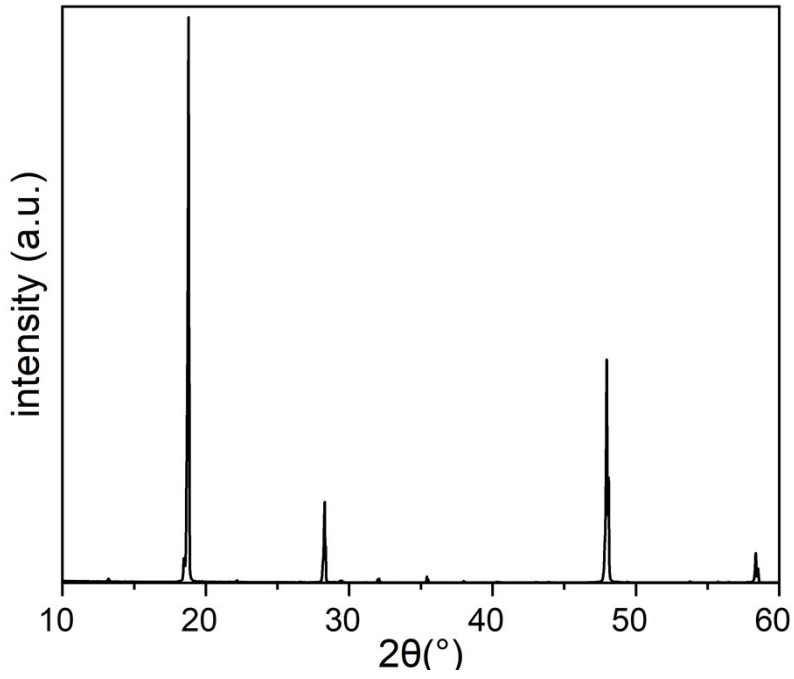

Figure S2. XRD pattern of $Bi_2Se_{2.33}S_{0.67}$.

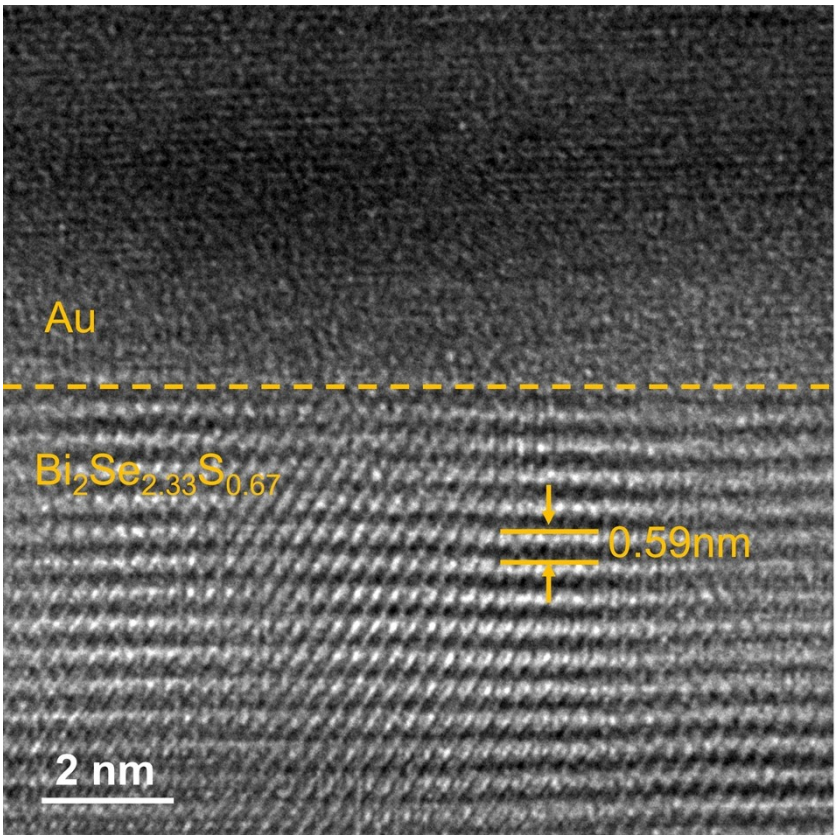

Figure S3. Cross-sectional HRTEM image of $Bi_2Se_{2.33}S_{0.67}$.

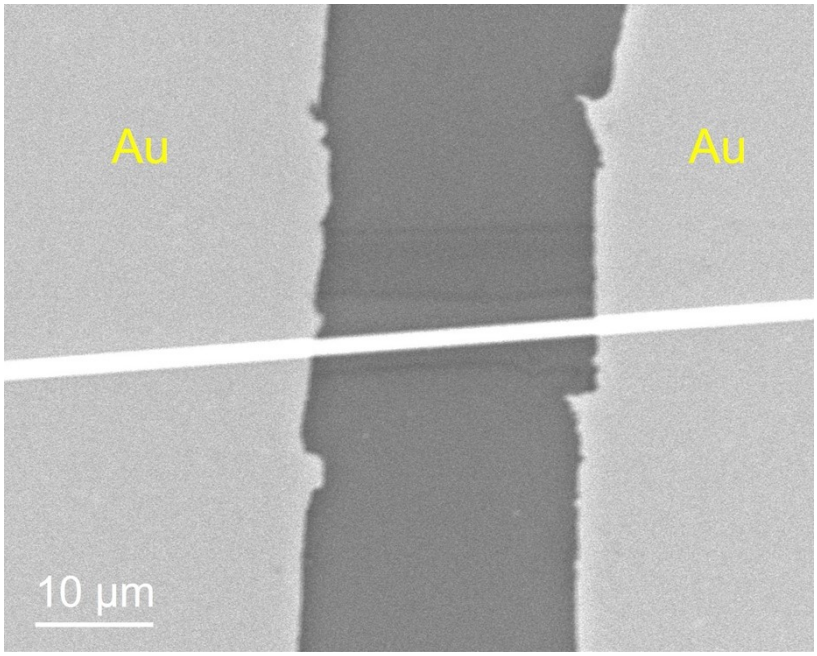

Figure S4. The scanning electron microscope image of a typical device.

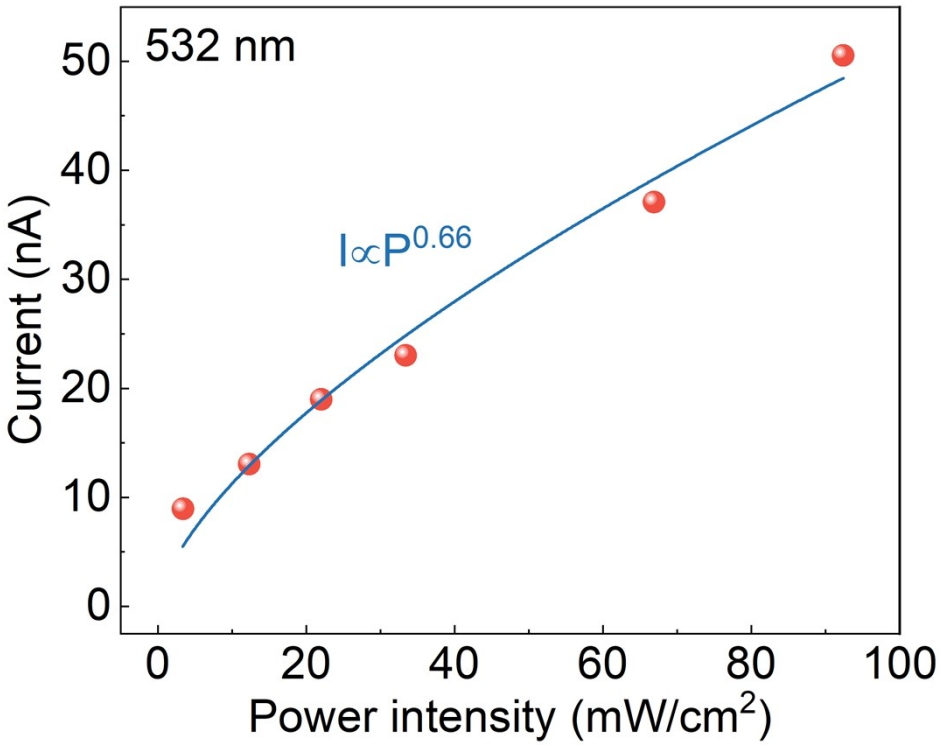

Figure S5. Current–power curves under light illumination of 532 nm of the $Bi_2Se_{2.33}S_{0.67}$ device.

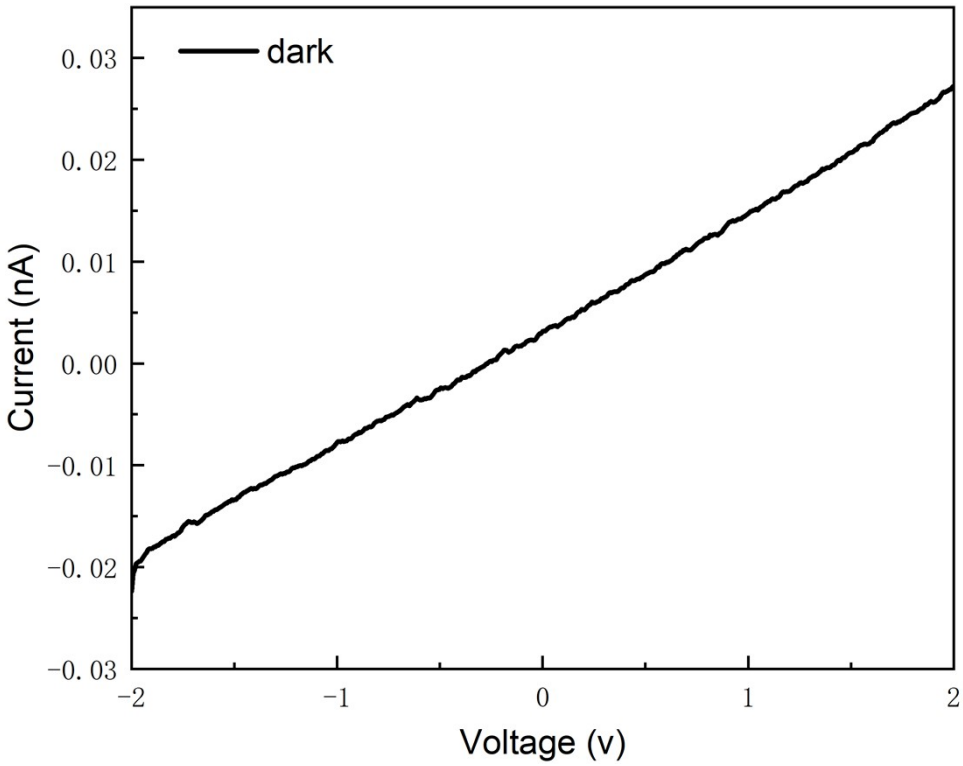

Figure S6. Dark current of the device.

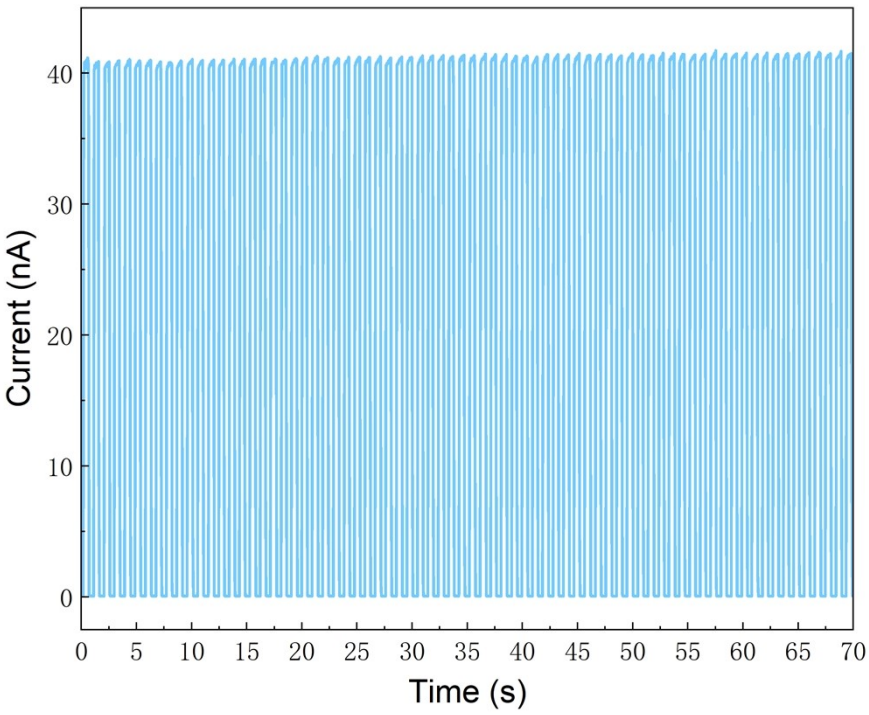

Figure S7. Time-resolved photoresponse at the irradiation of 532 nm light.

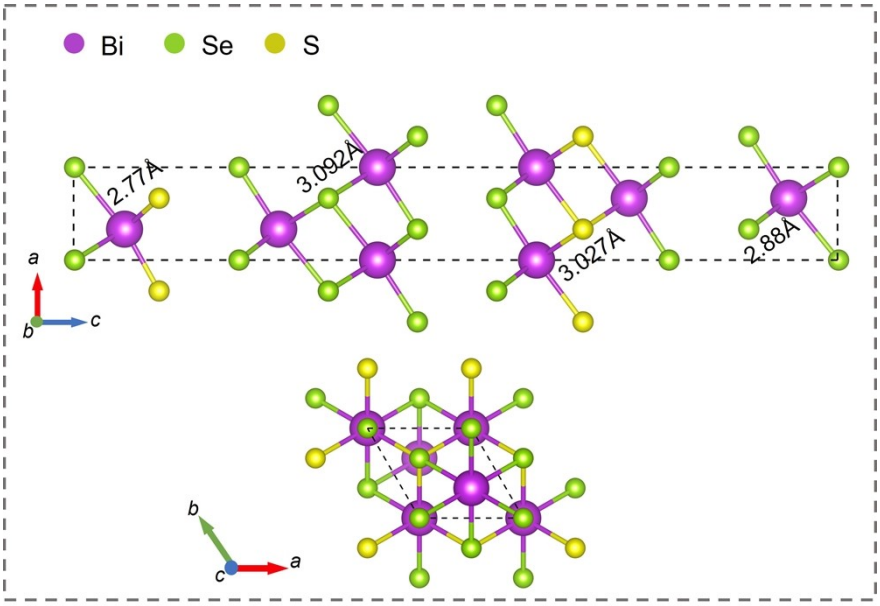

Figure S8. The $Bi_6Se_7S_2$ supercell structure.

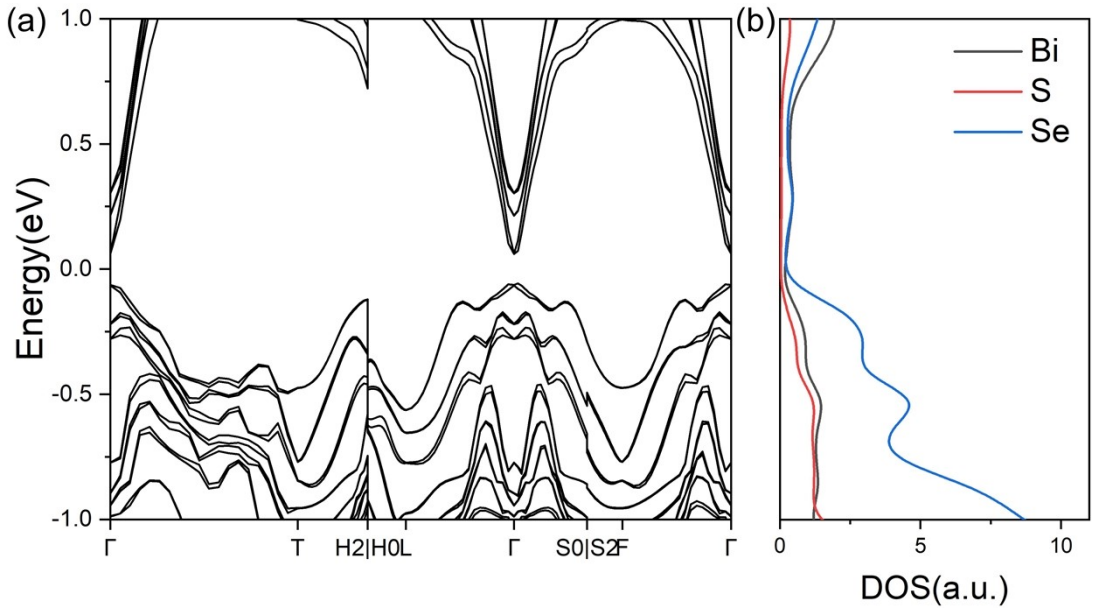

Figure S9. DFT calculations. (a) The band structure of $Bi_2Se_{2.33}S_{0.67}$. (b) Corresponding projected densities of states of $Bi_2Se_{2.33}S_{0.67}$.

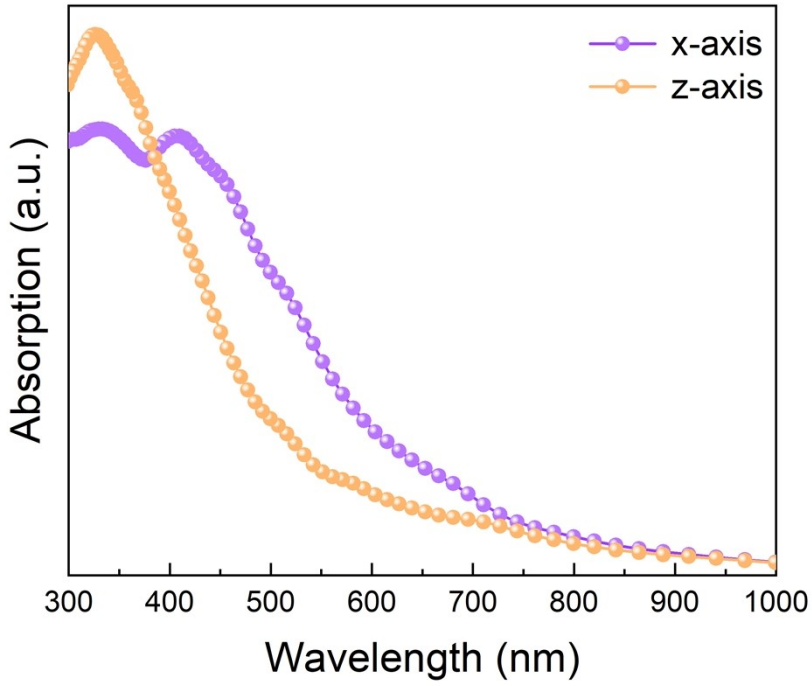

Figure S10. The calculated absorption spectra of $Bi_2Se_{2.33}S_{0.67}$ in the direction of x-axis and z-axis.

Table S1. Comparison of the photoresponse times with different materials.

Materials	Wavelength (nm)	Bias (V)	Response time	Reference
Bi_2Se_3	1456	1	0.54 s	[8]

Bi_2Te_3	1550	0.3	0.42 s	[9]
Bi_2S_3	532	2	20 ms	[10]
ZnO	370	5	0.1 ms	[11]
SnO_2	275	5	60 ms	[12, 13]
In_2S_3	450	1	6 ms	[14]
$Bi_2Se_{2.33}S_{0.67}$	532	1	364 ns	This Work

Table S2. Comparison of the photocurrent dichroic ratio with different materials.

Materials	Wavelength (nm)	Dichroic Ratio	Reference
2D SiP_2	365	1.6	[15]
MoS_2	660	1.45	[16]
$CH_3NH_3PbI_3$ NW	530	1.3	[17]
Cu_3PS_4 NW	520	1.3	[18]
Sb_2Se_3 NW	830	1.71	[19]
Layered NbS_3	830	1.84	[20]
Few-layer $GeAs_2$	532	1.9	[21]
ZnSb nanoplates	1550	1.58	[22]
$Bi_2Se_{2.33}S_{0.67}$	355	1.8	This Work

Reference

1. D. Hu, G. Xu, L. Xing, X. Yan, J. Wang, J. Zheng, Z. Lu, P. Wang, X. Pan and L. Jiao, *Angewandte Chemie International Edition*, 2017, **56**, 3611-3615.
2. P. E. Blöchl, *Physical Review B*, 1994, **50**, 17953-17979.
3. G. Kresse and J. Furthmüller, *Physical Review B*, 1996, **54**, 11169-11186.
4. G. Kresse and D. Joubert, *Physical Review B*, 1999, **59**, 1758-1775.
5. J. P. Perdew, K. Burke and M. Ernzerhof, *Physical Review Letters*, 1996, **77**, 3865-3868.
6. S. Grimme, *Journal of Computational Chemistry*, 2006, **27**, 1787-1799.
7. H. J. Monkhorst and J. D. Pack, *Physical Review B*, 1976, **13**, 5188-5192.
8. F. Wang, L. Li, W. Huang, L. Li, B. Jin, H. Li and T. Zhai, *Advanced Functional Materials*, 2018, **28**, 1802707.
9. A. Sharma, A. K. Srivastava, T. D. Senguttuvan and S. Husale, *Scientific Reports*, 2017, **7**, 17911.
10. W. Yang, J. Yang, K. Zhao, Q. Gao, L. Liu, Z. Zhou, S. Hou, X. Wang, G. Shen, X. Pang, Q. Xu and Z. Wei, *Advanced Science*, 2021, **8**, 2100075.
11. W. Wang, H. D. Xiong, M. D. Edelstein, D. Gundlach, J. S. Suehle, C. A. Richter, W.-K. Hong and T. Lee, *Journal of Applied Physics*, 2007, **101**, 044313.
12. S. Ju, P. Chen, C. Zhou, Y.-g. Ha, A. Facchetti, T. J. Marks, S. K. Kim, S. Mohammadi and D. B. Janes, *Applied Physics Letters*, 2008, **92**, 243120.
13. J. Yan, Y. Chen, X. Wang, Y. Fu, J. Wang, J. Sun, G. Dai, S. Tao and Y. Gao, *Nanoscale*, 2019, **11**, 2162-2169.
14. W. Huang, L. Gan, H. Yang, N. Zhou, R. Wang, W. Wu, H. Li, Y. Ma, H. Zeng and T. Zhai, *Advanced Functional Materials*, 2017, **27**, 1702448.

15. Z. Wang, P. Luo, B. Han, X. Zhang, S. Zhao, S. Wang, X. Chen, L. Wei, S. Yang, X. Zhou, S. Wang, X. Tao and T. Zhai, *ACS Nano*, 2021, **15**, 20442-20452.
16. S. Chen, R. Cao, X. Chen, Q. Wu, Y. Zeng, S. Gao, Z. Guo, J. Zhao, M. Zhang and H. Zhang, *Advanced Materials Interfaces*, 2020, **7**, 1902179.
17. L. Gao, K. Zeng, J. Guo, C. Ge, J. Du, Y. Zhao, C. Chen, H. Deng, Y. He, H. Song, G. Niu and J. Tang, *Nano Letters*, 2016, **16**, 7446-7454.
18. D. Kong, W. Dong, H. Yu, C. Zhao, Y. Zhao, Y. Yang, L. Fu, L. Jia, P. Wang, J. Liu, S. Zheng, Y. Xiong, R. Liu, Y. Zhou and J. Zhou, *Advanced Optical Materials*, 2024, **n/a**, 2402910.
19. S. Zhang, H. Wang, M. M. Kirchner, J. Liu, H. Luo, Y. Ren, C. Yuan, H. T. Hattori, A. E. Miroshnichenko and W. Lei, *Advanced Materials Interfaces*, 2022, **9**, 2200448.
20. Y. Wang, P. Wu, Z. Wang, M. Luo, F. Zhong, X. Ge, K. Zhang, M. Peng, Y. Ye, Q. Li, H. Ge, J. Ye, T. He, Y. Chen, T. Xu, C. Yu, Y. Wang, Z. Hu, X. Zhou, C. Shan, M. Long, P. Wang, P. Zhou and W. Hu, *Advanced Materials*, 2020, **32**, 2005037.
21. L. Li, P. Gong, D. Sheng, S. Wang, W. Wang, X. Zhu, X. Shi, F. Wang, W. Han, S. Yang, K. Liu, H. Li and T. Zhai, *Advanced Materials*, 2018, **30**, 1804541.
22. R. Chai, Y. Chen, M. Zhong, H. Yang, F. Yan, M. Peng, Y. Sun, K. Wang, Z. Wei, W. Hu, Q. Liu, Z. Lou and G. Shen, *Journal of Materials Chemistry C*, 2020, **8**, 6388-6395.